Theoretical

Toroidal Graphenes from 4-Valent Tori

Mircea V. Diudea

Faculty of Chemistry and Chemical Engineering
Babes-Bolyai University, 3400 Cluj, Romania
e-mail: diudea@chem.ubbcluj.ro

Bull. Chem. Soc. Japan, **2002**, *75*, 587-592

Square tori are transformed into hexagonal and other tiling tori by several cutting procedures. The toroidal objects thus generated are optimized by a molecular mechanics procedure. The strain energy, defined as the difference between the energy of toroidal structure and the energy of its corresponding straight, open tube, is shown to decrease as the torus diameter increases, in the series 10,*n* of polyhex tori, up to 5000 atoms. Graph-theoretical characterization of toroidal structures including the Hosoya polynomial, Distance Degree Sequence, and Wiener index is also given.

Running Title: Toroidal Graphenes from 4-Valent Tori

Graphene is a generic name for the carbon allotropes produced by laser vaporization of graphite. They include, besides the famous spherical fullerenes,[1-11] nanotubes, and their closed, circular forms with toroidal shape.

Nanotubes[12-14] produced in a carbon arc discharge belong to the same class of carbon allotropes as fullerenes. Toroidal nanotubes have also been reported[15-18] in the products of pure carbon laser vaporization and they strongly attracted the interest of scientists[19-35] since they could be ideal systems for studying interesting electronic and magnetic properties.[36,37]

Tubular graphenes are tessellated mainly by hexagons but incorporation of pentagons and heptagons into their hexagonal lattice is required for closing or getting suitable curvature.[35] Among the closed surfaces only tori and Klein bottles can be tiled by a pure polyhex net.[38]

A toroidal surface can be tiled with hexagons by cutting out a parallellogram[22,23,29,32,33] from a graphite sheet, rolling it up to form a tube and finally gluing its two ends to form a polyhex torus.

An alternative to the parallelogram procedure is the use of adjacency matrix eigenvectors in finding appropriate 3D coordinates of a graph (in particular, a torus).[39-41] The method was previously used in generating spheroidal fullerenes.[10] Polyhex tori are more acceptable to organic chemists (perhaps they offer the pure carbon benzenoid model[9,35]) while the other tiling tori (polygons smaller or larger than six) are expected to appear in supramolecular inorganic compounds (e.g., polyoxometalates[42])

Polyhex Tori from Square Tori

A torus $T_{c,n,C4}$ is a combinatorial torus tiled by quadrilaterals. In our procedure, the toroidal surface is generated according to an elementary geometry.[43] Next, a circulant *c*-folded cycle, lying in a plane perpendicular to the tube, runs along the torus. The *n* images of the circulant together with the edges joining (point by point) the subsequent images form a square lattice covering the torus. A simple transformation of the square net leads to a rhomboidal one.[44] Figure 1 illustrates a square torus $T_{8,12,C4}$ (a) and its rhomboidal transform (b).

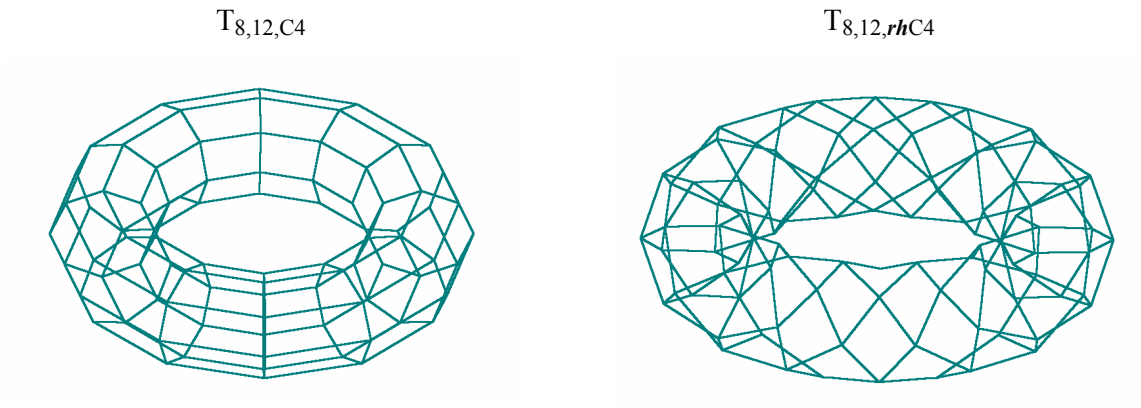

Fig. 1. Quadrilateral 4-valent tori

The main problem is to change the squares into hexagons or other tiling patterns, suitable from a chemical point of view. In this respect, we developed several cutting procedures.[45,46] For obtaining hexagonal patterns C_6, the cutting operation consists in deleting each second *horizontal* edge and alternating edges and cuts in each second row. It results in a *standard h,*C_6 *pattern* (Fig. 2, a). After optimization by a molecular mechanics program, a *phenanthrenoid* (i.e., zigzag) pattern appears on the torus (see below). The same algorithm, operating vertically, leads to a standard *v*,C_6 pattern (Fig. 2,b), meaning an *anthracenoid* (i.e., armchair) pattern. Figure 3 illustrates two such (optimized) tori.

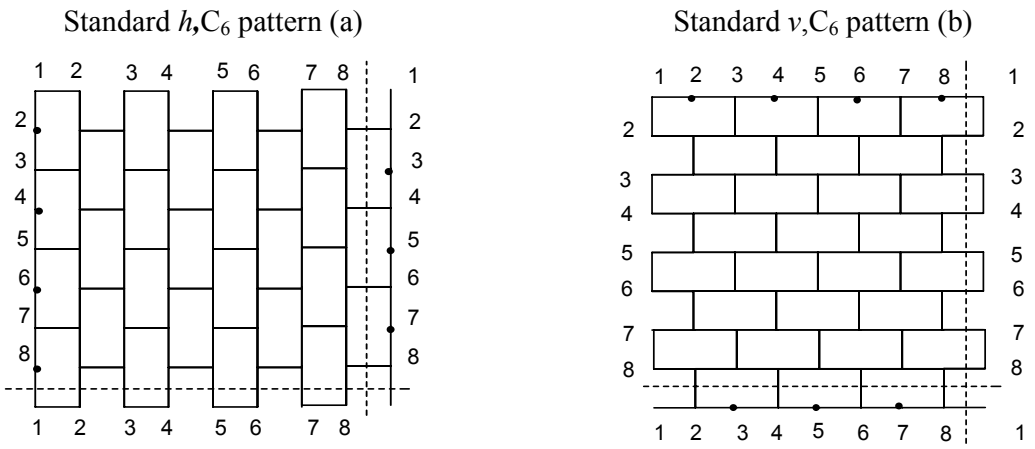

Fig. 2. Standard hexagonal patterns obtained by *h*-cutting (a) and *v*-cutting (b), respectively.

Note that each hexagon takes exactly two squares in the square lattice. As a consequence, the *number of hexagons is half the number of squares* in the torus T*c,n*: on dimension *c*, in case of *h*,C_6 *pattern* and dimension *n*, in case of *v*,C_6 *pattern*. Recall that the above cutting procedure *leaves unchanged the number of vertices in the original square torus*. The type of cutting (*h* or *v*) is added to the name of torus (see below). By varying the cutting algorithm, C_4,C_8, C_5,C_7 and C_5,C_6,C_7 patterns can be obtained.[45,46]

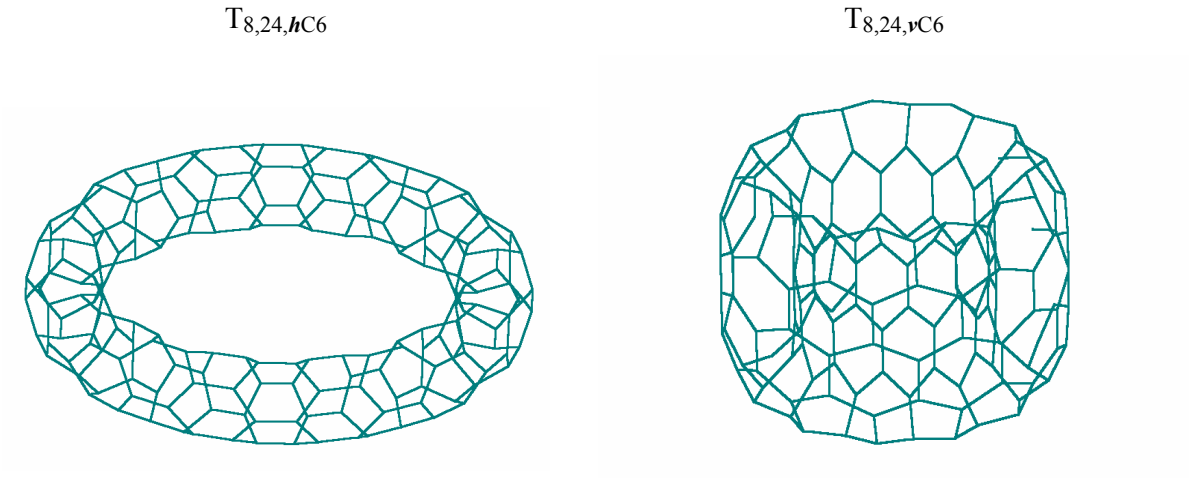

Fig. 3. A phenanthrenoid (zigzag) $T_{8,24,\boldsymbol{h}C6}$ and an anthracenoid (armchair) $T_{8,24,\boldsymbol{v}C6}$ toroidal graphene.

Energetics in Tori of C_6 10,*n* Series

In the observed "crop circles",[15] most of the individual tubes appear to be "perfect tori", free of topological pentagon-heptagon defects in their lattice, with no obvious kinks, created by these defects. Molecular mechanics studies performed by Han[47] (molecular systems from 2,000 up to 30,000 atoms, the torus diameters *D* of 60 nm and tube diameter *d* between 0.7 and 1.4 nm) showed that the defect-free circular tori are energetically stable structures. He stressed that the larger the diameter of the torus, the more energetically stable it is. A linear relation between the strain energy and $1/D^2$ has been obtained.

A simple observation that thinner tubes are more easily bent, together with studies on very thin tubes,[31] encouraged us to consider the series of tubes 10,*n* (*n* = 10, 20,...,500). The tubes of *h*-type (i.e., zigzag) show a width around 0.4 nm, while those of *v*-type (i.e., armchair) show a width about 0.7 nm. Their constitution, the number of atoms and the number of hexes along the torus, as well as their MM+ energy (in kcal/mol), are given in the Table. Note that the number of hexes across the tube is 5 and 10 for the *h*- and *v*-series, respectively. Also note that the "combinatorial" diameter *D* is obtained by dividing by *pi* the number of hexes along the torus. The ground data, given for tori and their corresponding open tubes, are further used for calculating the strain energy in tori. Figure 4 illustrates some representative members of the two sub-series.

$T_{10,200,\boldsymbol{h}C6}$ (outside) & $T_{10,200,\boldsymbol{v}C6}$ (inside) $T_{10,200,\boldsymbol{v}C6}$ (outside) & $T_{10,100,\boldsymbol{h}C6}$ (inside)

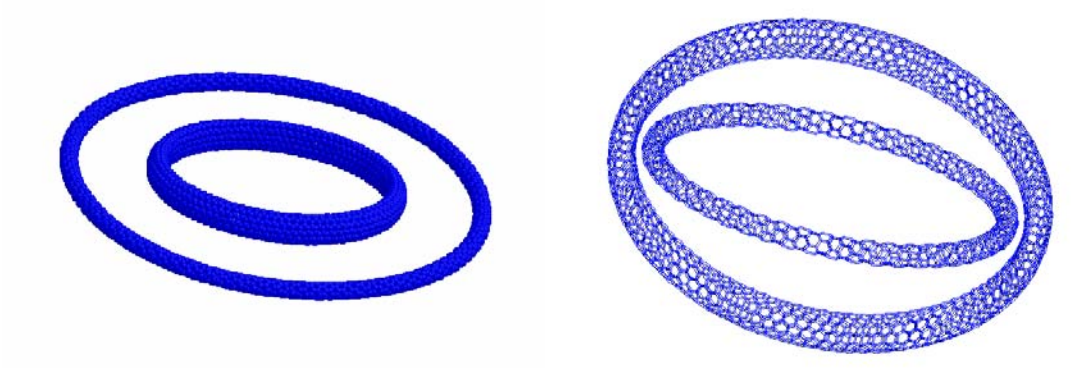

Fig. 4. Tori of C_6 10,*n* series.

Observe that, at $T_{10,200}$ level, the *h*-torus is twice as large (see also the Table) and twice as thin as the *v*-torus. In the *h*-series, the tube cross section, *elongated* at the beginning (see ref.[21]), becomes circular at $T_{10,100}$ level. In the *v*-series, (see Fig. 5) the cross section remains elongated up to $T_{10,400}$ but it becomes circular at $T_{10,500}$ level (i.e., 5000 atoms and 250 hexes along the torus).

The strain energy is herein defined as the difference between the MM+ energy of the torus and its corresponding open tube. Since the linear relation between MM+ energy and constitution is almost perfect within this series (see footnotes of the Table), we used it in calculating the energy for tubes with $n > 100$. Figure 6 illustrates the trend of the strain energy in the above series.

Table. Number of Hexes along the Torus and MM+ Energy in Tori and Tubes of C_6 10,*n* Series.

No. atoms	*h*_Hexes	Energy/kcal·mol^{-1}		No. atoms	*v*_Hexes	Energy/kcal·mol^{-1}	
		*h*_Tori	*h*_Tubes			*v*_Tori	*v*_Tubes
100	10	6631.2	717.16	100	5	9722.51	178.31
200	20	3979.99	1465.98	200	10	6831.24	371.04
300	30	4119.42	2216.16	300	15	5961.02	564.08
400	40	4505.69	2963.93	400	20	5500.53	756.6
500	50	5018.45	3712.96	500	25	5225.93	949.31
600	60	5597.65	4461.25	600	30	5084.6	1141.93
700	70	6217.51	5210.66	700	35	5029.93	1336.13
800	80	6856.54	5962.41	800	40	5033.92	1527.56
900	90	7517.13	6710.48	900	45	5078.13	1722.46
1000	100	8193	7459.01	1000	50	5150.04	1917.15
1100	110	8881.04	8207.725*	1100	55	5243.29	2109.133**
1200	120	9580.29	8956.775*	1200	60	5351.65	2302.333**
1300	130	10286.62	9705.825*	1300	65	5471.02	2495.533**
1400	140	10994.8	10454.88*	1400	70	5599.11	2688.733**
1500	150	11714.03	11203.93*	1500	75	5734.46	2881.933**
1600	160	12434.14	11952.98*	1600	80	5876.1	3075.133**
1700	170	13162.77	12702.03*	1700	85	6021.43	3268.333**
1800	180	13881.11	13451.08*	1800	90	6169.54	3461.533**
1900	190	14615.64	14200.13*	1900	95	6322.15	3654.733**
2000	200	15401.39	14948.67	2000	100	6477.45	3848.58
2500	250	19022.67	18694.43*	3000	150	7928.85	5779.933**
				4000	200	9379.34	7711.933**
				5000	250	10990.92	9643.933**

* Calculated by eq: Energy = 74.905x - 31.825; $R^2 = 1$.
** Calculated by eq: Energy = 38.64x - 16.067; $R^2 = 1$.

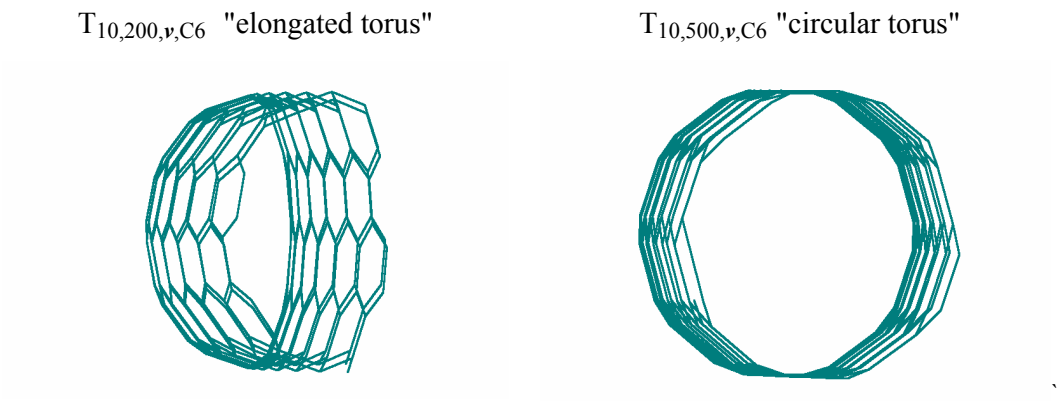

Fig. 5. Cross sections in "elongated" and "circular" tori, respectively.

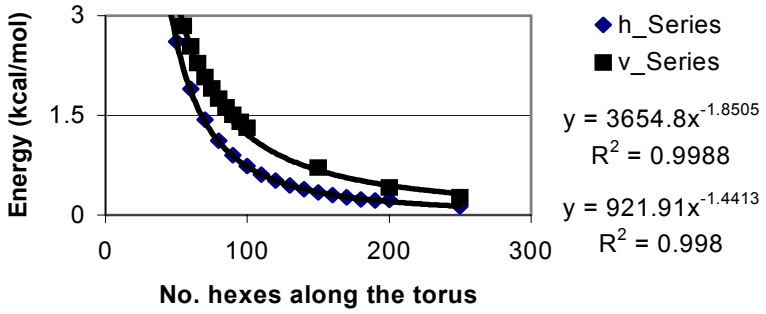

Fig. 6. Strain energy/atom in tori of C_6 10,*n* series.

Note that, at the same number of hexes along the torus, the strain energy is higher for the *v*-series than for the *h*-series. This is just the expected trend, keeping in mind the tori constitution. The dependency on the torus diameter is: Strain energy = 439 $D^{-1.8505}$ (*h*-series) and 177.07 $D^{-1.4413}$ (*v*-series), with the same R^2 as shown in Fig. 6.

The fact that the "elongated" [21] tori represent the major population in our series explains the departure from the Han's trend of D^{-2} obtained for large circular tori.

At the end of this section we can say that the series of thin tori herein discussed appear as possible graphenes, to be found among the graphite laser vaporization products.

Topological Characterization of Polyhex Tori

In 1988 Hosoya proposed a novel graphical polynomial,[48] defined as:

$$H(G,x) = \sum_{k=0}^{d(G)} d(G,k)x^k \qquad (1)$$

with $d(G,0) = v$ and $d(G,1) = e$. In the above relations, v is the number of vertices in the graph G, e the number of edges, $d(G)$ the topological diameter (i.e., the longest topological distance in G) and $d(G,k)$ the number of pair vertices lying at distance k of each other. The polynomial (called Wiener, by its author but Hosoya in the more recent literature[49]) can be expressed as a function of the vertex contributions $H(i,x)$:

$$H(i,x) = \sum_{k=0}^{d(G)} d(i,k)x^k \qquad (2)$$

where $d(i,k)$ is the number of vertices at distance k from the vertex i. Keeping in mind that each path has two endpoints (i.e., each path is counted twice), it becomes clear that, in a vertex transitive graph, the following relation holds (see also ref.[49]):

$$vH(i,x) = 2H(G,x) - v \qquad (3)$$

The general form of the vertex Hosoya polynomials, for tori of type $T_{c,n,h,C6}$ and $T_{c,n,v,C6}$, (regular graphs, having $v = cn$), in going from normal h,C_6 to normal v,C_6 tori, is:

$T_{c,n,h,C6;}\ n > c$:

$$H(i,x) = 1 + 3kx^k{}_{,k=1,2,...,(c/2-1)} + (3c/2-1)x^{c/2} + (3c/2-k)x^{(c/2+k)}{}_{,k=1,2,...,(c/2-1)} + \\ + cx^k{}_{,k=c,c+1,...,(n-1)} + (c/2)x^n \qquad (4)$$

$T_{c,n,h,C6} = T_{c,n,v,C6;}\ n = c$:

$$H(i,x) = 1 + 3kx^k{}_{,k=1,2,...,(c/2-1)} + (3c/2-1)x^{c/2} + (3c/2-k)x^{(c/2+k)}{}_{,k=1,2,...,(c/2-1)} + \\ + (c/2)x^n \qquad (5)$$

$T_{c,n,v,C6;}\ c+2 \le n \le 2(c-1)$:

$$H(i,x) = 1 + 3kx^{k}{}_{,k=1,2,\ldots,(n/2-1)} + (3n/2-1)x^{n/2} + (3n/2-k)x^{(n/2+k)}{}_{,k=1,2,\ldots,(c-1-n/2)} + \\ + (2n-3c/2-1)x^{c} + [2(n-c)-4k]x^{(c+k)}{}_{,k=1,2,\ldots,((n-c)/2-1)} + x^{(c+n)/2} \quad (6)$$

$T_{c,n,v,C6;}\ n = 2c$:

$$H(i,x) = 1 + 3kx^{k}{}_{,k=1,2,\ldots,(c-1)} + (5c/2-2)x^{c} + (2c-4k)x^{(c+k)}{}_{,k=1,2,\ldots,(c/2-1)} + x^{(c+n)/2} \quad (7)$$

$T_{c,n,v,C6;}\ n \ge 2(c+1)$:

$$H(i,x) = 1 + 3kx^{k}{}_{,k=1,2,\ldots,(c-1)} + (5c/2-1)x^{c} + 2cx^{k}{}_{,k=c+1,c+2,\ldots,(n/2-1)} + (2c-1)x^{n/2} + \\ + (2c-4k)x^{(n/2+k)}{}_{,k=1,2,\ldots,(c/2-1)} + x^{(c+n)/2} \quad (8)$$

"Normal" torus, in the above, means a toroidal net having a number of hexes on the tube smaller than that around the torus. The "normal" status is already reached at $n > c$, in h,C_6 tori, while $n \ge 2(c+1)$ is needed in the case of v,C_6 tori.

Note that the coefficients of the vertex Hosoya polynomial are just the entries in the LC matrix (i.e., Layer matrix of Cardinality)[50] or the (vertex) Distance Degree Sequence DDS(i) (i.e., the number of vertices lying at distance k from the vertex i).[51] Clearly, the vertex decomposition of $H(G,x)$ would be more complicated in vertex non-transitive graphs.

The polynomial coefficients can be viewed as a "distance degree" spectrum, useful in topological characterization of graphenes. In the case of the (normal) C_6 10,n series, the spectra are shown in Fig. 7.

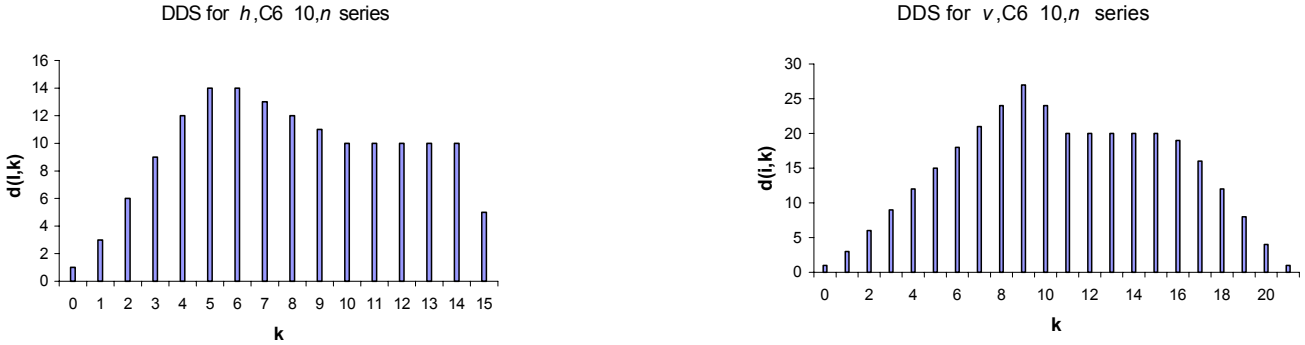

Fig. 7. Distance Degree Sequences DDS of C_6 10,n series.

The repeating terms : $cx^k{}_{,k=c,c+1,\ldots,n-1}$ and $2cx^k{}_{,k=c+1,c+2,\ldots,n/2-1}$, respectively, are the only changes, as *n* increases, in the spectrum of a given series (i.e., a series of fixed *c*). If one changes the series, the spectrum will drastically change, according to the general formulas (4) -(8).

The first derivative[52] of the Hosoya polynomial (for $x = 1$) equals the well-known Wiener[53] number *W* (i.e., the sum of all distances in *G*): $W = H'(G,1)$ [48].

In case of the normal series of tori, the first derivative of the Hosoya polynomial leads to:

$T_{c,n,h,C6}$:

$$W = \frac{nc}{2}\left[\sum_{k=1}^{c/2-1} 3k^2 + (3c/2-1)c/2 + \sum_{k=1}^{c/2-1}(3c/2-k)(c/2+k) + \sum_{k=c}^{n-1} ck + nc/2\right] \quad (9)$$

$T_{c,n,v,C6}$:

$$W = \frac{nc}{2}\left[\sum_{k=1}^{c-1} 3k^2 + (5c/2-1)c + \sum_{k=c+1}^{n/2-1} 2ck + (2c-1)n/2 + \sum_{k=1}^{c/2-1}(2c-4k)(n/2+k) + (n/2+c/2)\right] \quad (10)$$

By expanding the sums one obtains:

$T_{c,n,h,C6}$: $$W = \frac{1}{24}nc^2(6n^2 + c^2 - 4) \quad (11)$$

$T_{c,n,v,C6}$: $$W = \frac{1}{24}nc^2(3n^2 + c^2 + 3nc - 4) \quad (12)$$

Expansion of eq. 6 (case v,C_6; $c+2 \le n \le 2(c-1)$) also leads to relation (12). Moreover, the formulas for the other two cases:

$n = c$:

$$W = \frac{c^3}{24}(7c^2 - 4) \quad (13)$$

and

$n = 2c$: $$W = \frac{c^3}{12}(19c^2 - 4) \quad (14)$$

can be deduced from the first derivative of the corresponding polynomials (eqs. 5 and 7, respectively), as well as from eq. 12. Relation (13) is also a particular case of eq. (11), proving the selfconsistency of the formulas (eqs. 11 and 12) for calculating the Wiener index in polyhex tori.

Conclusion: the generation of toroidal polyhex graphenes from the 4-valent square tori is a very simple and reliable method. The resulting tori are characterized by only two topological parameters: *c* (c-folding of the tube) and *n* (n-folding of the torus). They are further optimized by an MM procedure. The strain energy in the 10,*n* series appears to decrease as the torus diameter increases. The topology of the polyhex net of these graphenes can be characterized by the Hosoya polynomial, distance degree spectra and Wiener number.

References

1. H. Kroto, *Fullerene Sci. Technol*., **2**, 333-342 (1994).
2. F. Diedrich and C. Thilgen, *Science*, **271,** 317-323 (1996).
3. H. Zorc, Lj. P. Toli, S. Martinovi, and D. Srzi, *Fullerene Sci. Technol.*, **2**, 471-480 (1994).
4. I. S. Neretin, K. A. Lyssenko, M. Yu. Antipin, Yu. L. Slovokhotov, O. V. Boltalina, P. A. Troshin, A. Yu. Lukonin, L. N. Sidorov, and R. Taylor, *Angew. Chem., Int. Ed.*, **39**, 3273-3276 (2000).
5. W. Rubin and Y. Qian, *Angew. Chem., Int. Ed*., **39**, 3133-3137 (2000).
6. K. Lee, Ch. H. Lee, H. Song, J. T. Park, H. Y. Chang, and M.-G. Choi, *Angew. Chem., Int. Ed*., **39**, 1801-1804 (2000).
7. T. F. Fässler, R. Hoffmann, S. Hoffmann, and M. Wörle, *Angew. Chem., Int. Ed*., **39,** 2091-2094 (2000).
8. M. Menon, E. Richter, and K. R. Subbaswamy, *Phys. Rev. B*, **57**, 4063-4066 (1998).
9. T. G. Schmalz, W. A. Seitz, D. J. Klein, and G. E. Hite, *J. Am. Chem. Soc.,* **110**, 1113-1127 (1988).
10. D. E. Manolopoulos and P. W. Fowler, *J. Chem. Phys.,* **96**, 7603-7614 (1992).
11. G. Brinkmann, P. W. Fowler, and M. Yoshida, *Commun. Math. Comput.*

Chem. (*MATCH*), **38**, 7-17 (1998).

12. S. Iijima, *Nature*, **354**, 56-58 (1991).

13. S. Iijima and T. Ichihashi, *Nature,* **361**, 603-605 (1993).

14. A. L. Ivanovskii, *Russ. Chem. Rev.*, **68**, 103-118 (1999).

15. J. Liu, H. Dai, J. H. Hafner, D. T. Colbert, R. E. Smalley, S. J. Tans, and C. Dekker, *Nature*, **385**, 780-781 (1997).

16. R. Martel, H. R. Shea, and P. Avouris, *Nature,* **398**, 299-299 (1999).

17. R. Martel, H. R. Shea, and P. Avouris, *J. Phys. Chem. B*, **103**, 7551-7556 (1999).

18. M. Ahlskog, E. Seynaeve, R. J. M. Vullers, C. Van Haesendonck, A. Fonseca, K. Hernadi, and J. B. Nagy, *Chem*. *Phys. Lett*., **300**, 202-206 (1999).

19. S. Itoh and S. Ihara, *Phys. Rev*. *B*, **47**, 1703-1704 (1993).

20. S. Ihara and S. Itoh, *Phys. Rev*. *B*, **47**, 12908-12911 (1993).

21. S. Itoh and S. Ihara, *Phys. Rev*. *B*, **48**, 8323-8328 (1993).

22. E. C. Kirby, *Croat. Chem. Acta*, **66**, 13-26 (1993).

23. E. C. Kirby, R. B. Mallion, and P. Pollak, *J. Chem. Soc., Faraday Trans*., **89**, 1945-1953 (1993).

24. S. Itoh and S. Ihara, *Phys. Rev*. *B*, **49**, 13970-13974 (1994).

25. J. K. Johnson, B. N. Davidson, M. R. Pederson, and J. Q. Broughton, *Phys. Rev*. *B*, **50**, 17575-17582 (1994).

26. B. Borštnik and D. Lukman, *Chem. Phys*. *Lett.*, **228** 312-316 (1994).

27. E. C. Kirby, *Fullerene Sci*. *Technol*., **2**, 395-404 (1994).

28. J. E. Avron and J. Berger, *Phys. Rev*. *A*, **51**, 1146-1149 (1995).

29. P. E. John, *Croat. Chem. Acta,* **71**, 435-447 (1998).

30. V. Meunier, Ph. Lambin, and A. A. Lucas, *Phys. Rev*. *B*, **57**, 14886-14890 (1998).

31. D-H. Oh, J. M. Park, and K. S. Kim, *Phys. Rev*. *B*, **62**, 1600-1603 (2000).

32. A. Ceulemans, L. F. Chibotaru, S. A. Bovin, and P. W. Fowler, *J. Chem. Phys*., **112**, 4271-4278 (2000).

33. D. Marušić and T. Pisanski, *Croat. Chem. Acta*, **73**, 969-981 (2000).

34. S. A. Bovin, L. F. Chibotaru, and A. Ceulemans, *J. Mol. Catalysis*, *A*, **166**, 47-52 (2001).

35. D. Babić, D. J. Klein, and T. G. Schmalz, *J. Mol. Graphics Modell.*, **19**, 222-231 (2001).

36. M. F. Lin and D. S. Chuu, *Phys. Rev. B*, **57**, 6731-6737 (1998).

37. A. Ceulemans, L. F. Chibotaru, and P. W. Fowler, *Phys. Rev. Lett*., **80**, 1861-1864 (1998).

38. E. C. Kirby and T. Pisanski, *J. Math. Chem*. **23**, 151-167 (1998).

39. A. Graovac, D. Plavšić, M. Kaufman, T. Pisanski, and E. C. Kirby, *J. Chem. Phys.*, **113**, 1925-1931 (2000).

40. A. Graovac, M. Kaufman, T. Pisanski, E. C. Kirby, and D. Plavšić, *J. Chem. Phys.,* **113**, 1-7 (2000).

41. I. Laszlo, A. Rassat, P. W. Fowler, and A. Graovac, *Chem. Phys. Lett*., **342**, 369-374 (2001).

42. A. Muller, P. Kogerler, and Ch. Kuhlman, *Chem. Commun*., 1347-1358 (1999).

43. M. V. Diudea and A. Graovac, *Commun. Math. Comput. Chem.* (*MATCH*), **44**, 93-102 (2001).

44. M. V. Diudea and P. E. John, *Commun. Math. Comput. Chem*. (*MATCH*), **44**, 103-116 (2001).

45. M. V. Diudea, I. Silaghi-Dumitrescu, and B. Parv, *Commun. Math. Comput. Chem.* (*MATCH*), **44**, 117-133 (2001).

46. M. V. Diudea and E. C. Kirby, *Fullerene Sci. Technol*. 9, 445-465 (2001).

47. J. Han, *Chem. Phys. Lett*., **282**, 87-191 (1998).

48. H. Hosoya, *Discrete Appl. Math*., **19**, 239-257 (1988).

49. I. Gutman, S. Klavžar, M. Petkovšek, and P. Žigert, *Commun. Math. Comput. Chem*. (*MATCH*), 43, 49-66 (2001).

50. M. V. Diudea, *J. Chem. Inf. Comput. Sci.,* **34**, 1064-1071 (1994).

51. M. V. Diudea, I. Gutman, and L. Jäntschi, "*Molecular Topology",* Nova Science, Huntington, New York (2001).

52. E. V. Konstantinova and M.V. Diudea, *Croat. Chem. Acta,* **73**, 383-403 (2000)

53. H. Wiener, *J. Am. Chem. Soc.,* **69**, 17-20 (1947).